PROCEEDINGS, Thirty-First Workshop on Geothermal Reservoir Engineering
Stanford University, Stanford, California, January 30-February 1, 2006
SGP-TR-179

DESIGN AND ANALYSIS OF KIZILCAHAMAM TRACER TEST

Tevfik Kaya[1], Serhat Akin[1], Mahmut Parlaktuna[1] and Simeon Kostyanev[2]

[1]Petroleum & Natural Gas Engineering Department
Middle East Technical University
06531 Ankara - Turkey
e-mail: serhat@metu.edu.tr

[2]The Bulgarian Academy of Sciences
Geographical institute,
Sofia – 1113, Bulgaria

ABSTRACT

Kizilcahamam is a low temperature (~ 80°C) geothermal field located 70 km far from Ankara, Turkey. The produced geothermal water is used to heat more than 2500 houses. In order to characterize the reservoir a tracer-test was planned using the efficient hydrologic tracer-test design technique. The test was carried out by injecting a slug of fluorescein from a shallow re-injection well. The analysis results showed that the injection well and the producers are interconnected. Analysis of time-concentration curves showed that multi-fracture model represented the multi-peaked curves better than the others including homogeneous porous and double porosity models. The results are consistent with the conceptual geological models proposed in the literature.

INTRODUCTION

Kızılcahamam geothermal field is located 70km far from Ankara (Fig. 1). The geothermal fluid, produced with an average temperature of 74–86°C (Gevrek, I, 2000) and flowrate of 80 l/s is used in 2500 house district heating, in thermal hotels (Başkent University Thermal Hotel, Asya Thermal Resorts, Ab-ı Hayat and municipality hotels), in district facilities by using heat exchangers (Kaya, 2005). Used geothermal water is reinjected to the reservoir with a flowrate of 40 l/s at a temperature of approximately 42°C in a shallow and a deep reinjector. A total of 6 production and 2 reinjector wells are currently present in the field (Fig. 2). Deep reinjector well (KHD-1) is used as a production well during winters. All production wells use pumps at depths between 50 and 66 meters (Table 1). The objective of this study is to characterize and describe a tracer test conducted recently. First the geology and current situation of the field will be described. The tracer test design and its evaluation will then be given. The paper will be finished with conclusions.

Table 1. Producing and injecting well properties.

Name of the Well	Well Depth (m)	Flow rate (l/s)	Well head temperature (°C)	Dynamic Level (m)	Pump depth (m)
MTA-1(re-injection)	179	40	42	0	0
MTA-2	310	30	76	120	65
KHD-1(re-injection)	1556	15	42	0	0
İHL-1	590	20	76	25	65
İHL-2	670	40	74	30	66
İHL-3	673	20	79	20	57
FETHIBEY	592	20	76	25	65
Asya Finans	600	20	65	25	50

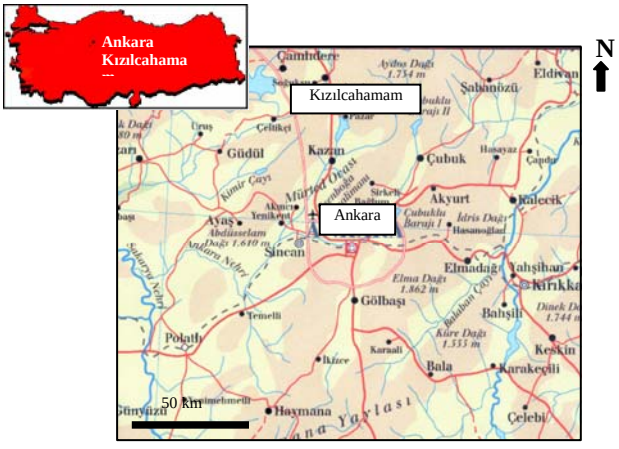

Figure. 1. Kizilcahamam geothermal field location map.

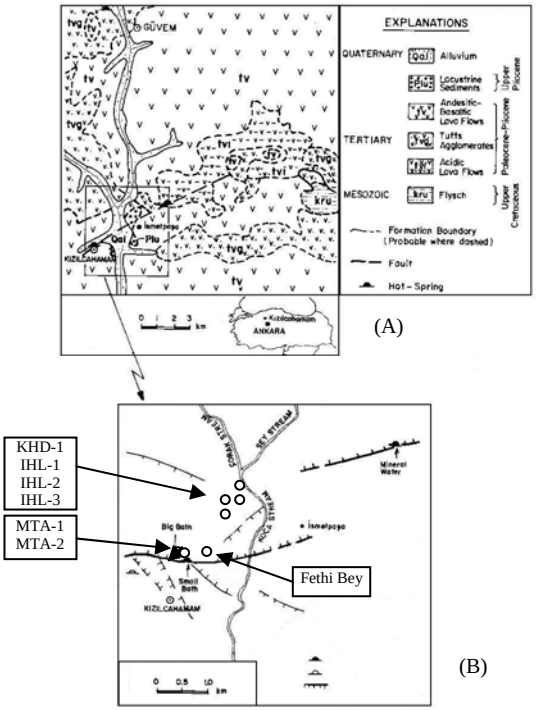

Figure. 2. (A) Geological map of Kızılcahamam area (Erol, 1955), (B) Location of wells in Kızılcahamam Geothermal Field (Revised from Özbek, 1988).

Geology

Geological, geochemical and geophysical studies have been previously carried out by Tatli (1975), Ongur (1976), Kocak (1977), Demirorer (1985), Gurer and Celik (1987), Gevrek and Aydin (1988), Ozbek (1988) and Gulec (1994). The Kızılcahamam area is located within the Tertiary-aged Galatian Volcanic Province that consists of autoclastic and pyroclastic deposits (Gevrek, 2000). Stratigraphic units (approximately 1800 m) from the bottom to the top are as follows: 1. Basaltic lava flows (Paleocene); 2. Pyroclastic deposits consisting of tuffs and agglomerates (Miocene); 3.Undifferentiated lava flows ranging in composition from andesitic, basaltic, trachyandesitic to dacitic (Miocene); 4.Debris flows (Quaternary) (see KHD-1 stratigraphic section in Fig. 4). The basement beneath the province consists of Paleozoic schists and Permo-Triassic limestones. The Lower Cretaceous limestone and Upper flysch facies and limestone lie over the Paleozoic basement, and are overlain by the Galatian Volcanic Province. The volcanic activity is believed to have started at the end of the Upper Cretaceous, but reached its climax during the Miocene age (Gevrek, 2000). Gravity faults, which strike dominantly in the ENE–WSW direction, are observed in the district. The Kızılcahamam fault, which passes through the town has approximately an E–W direction and is 2250 m in length (Fig. 3).

Chemical Properties of Geothermal Fluid

Thermal waters issuing through the Tertiary aged volcanics in the Kizilcahamam geothermal area are all alkali-bicarbonate waters with temperatures ranging from 28°C to 86°C. The waters from the town center have the highest temperature and an intermediate total dissolved solid content, in comparison to the waters sampled from the localities outside the town center. The Kızılcahamam geothermal water has a pH of approximately 7.2. It contains bicarbonate, chlorite, sodium, carbon dioxide and arsenic. The water is suitable for balneology and Kızılcahamam thermal water has solution mineral value of 250mg/l. The chemical classification is; bicarbonate (67.18%), chlorite (19.22%), sodium (82.64%), arsenic (0.34 mg/l) and carbon dioxide (283.4 mg/l). Metaboric acid (18.95 mg/l) and fluorite (1.96 mg/l) also exist (Kaya, 2005). The variations in the temperature and the chemical composition of the waters can be accounted for by a combination of processes including mixing between cold-shallow and hot-deep waters, boiling either before or after mixing, steam heating and conductive cooling. The chemical geothermometers, silica-enthalpy and enthalpy-chloride mixing models suggest a reservoir temperature of 124–190°C for the Kizilcahamam region, and a maximum of 71% deep, hot component for the thermal waters (Gulec, 1994).

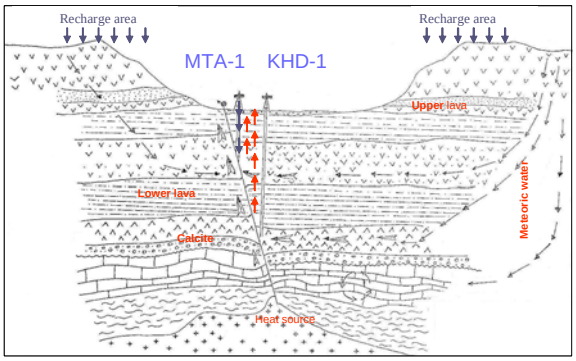

Figure. 3. Conceptual model of Kizilcahamam geothermal field.

Production, Temperature and Pressure Analysis

Figures 5 through 7 gives the cumulative production and re-injection, temperature and average dynamic level history for each well,. As can be seen from these figures MTA-1 well produced up to July 98 and then started re-injection of the used geothermal fluid as of winter 98. During summers only MTA-2 operates and that's why flat production is observed in other wells. Total production – re-injection ratio was found as 3.2 (Fig. 5). This ratio is relatively high for a low temperature geothermal field and this shows that pressure decline is more than it should be (See for example Fig. 7). Thus, this ratio has to be reduced to a smaller number (for example 1.5) for

good pressure support and efficient management of the field.

Temperature measurements of the wells are given in Fig. 6. MTA-1 well was used as production well up to July 98 after this date re-injection started. The well head temperature was 75-80°C before start to re-injection but dropped to 42°C after re-injection. It can be observed that temperature increased when a well was shut-in during summer. Temperature of the field seems to be not affected by re-injection with the exception of IHL-1. Since, IHL-1 is a production well which is not near to a re-injection well such temperature drops are not expected. This drop may result due to fresh and cold water intrusion in to the well possibly due to a mechanical failure such as cement bond or casing / liner failure(s).

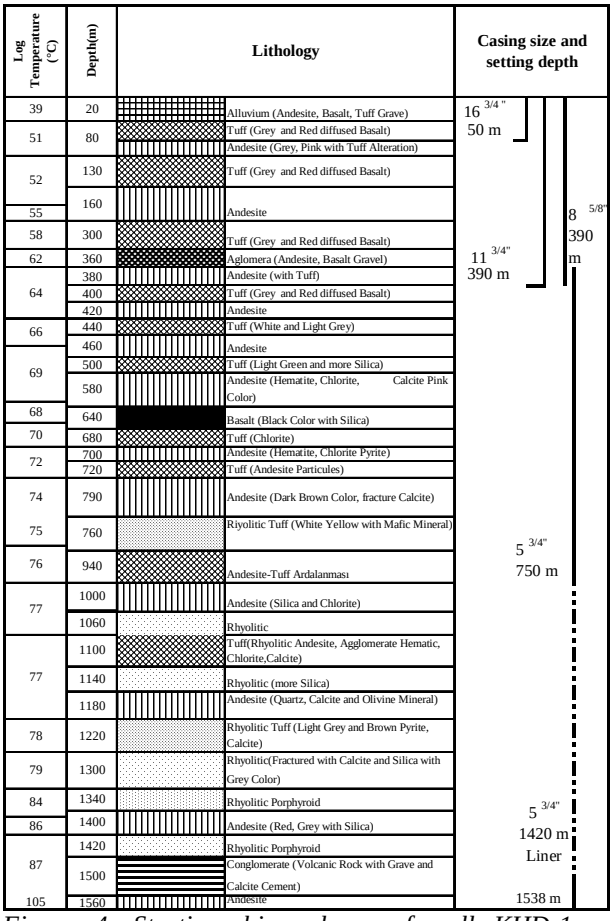

Figure 4. Stratigraphic column of well KHD-1, Kizilcahamam Geothermal Field (Kaya, 2005)

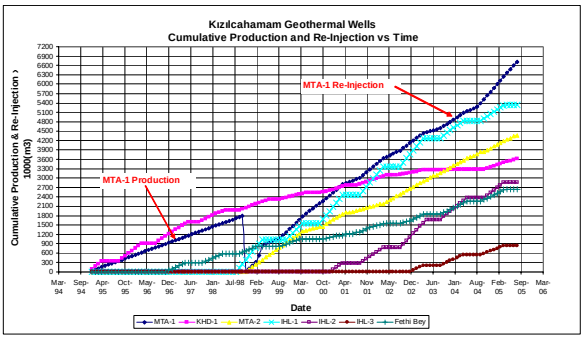

Figure 5. Production – re-injection history of wells in Kizilcahamam Geothermal Field (Kaya, 2005)

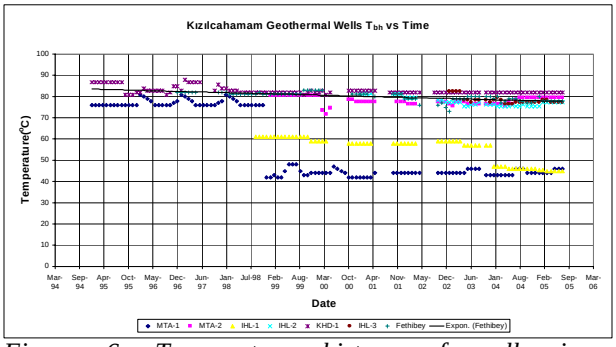

Figure 6. Temperature history of wells in Kizilcahamam Geothermal Field (Kaya, 2005)

Pressure declines observed in the field (Fig. 7) suggest that in 2011, the pump setting depths must be increased. Yet another strategy to maintain the dynamic levels is to decrease the total production – re-injection ratio. One final solution could be the change of re-injection location for better pressure support.

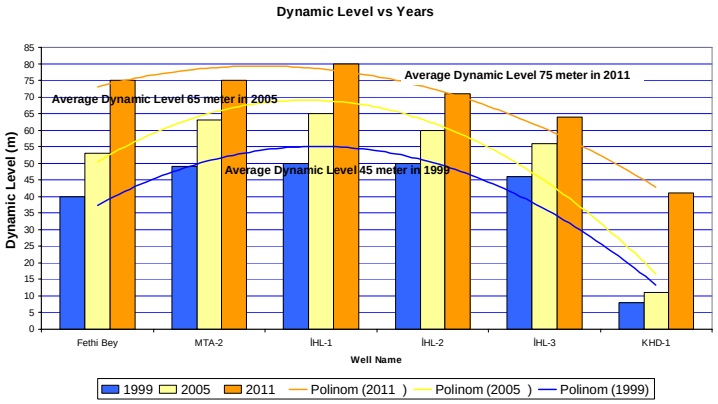

Figure 7. Pressure profile of wells in Kizilcahamam Geothermal Field at different times (Kaya, 2005)

TRACER TEST DESIGN

In order to determine the amount of fluoreiscein to be mixed in the geothermal fluid in re-injection well, a literature survey was conducted and 33 design methods were determined. Most of the methods are empirical equations that depend on the chemicals used in the tracer test, the formation of injection (karst, sandstone, etc.) and fractured or not and the permeability of the formation. In these methods, the main aim is to determine the amounts of the chemicals used in injection fluid. For example, Kilpatrick (1993) offered to use M (mass) = V(volume) / 200 in order to determine the mass of the tracer. Field (2003) observed that most design methods are applicable for only one chemical (like fluorescein) or one formation type (i.e, fractured, karstic, etc). The design equations are usually functions of flow rate, the distance between the wells and time.

The most complex part of the tracer test is the determination of the sampling frequency in the investigation well. To determine the sampling frequency two basic methods are offered; the methods that depend on the samples of the tracer tests, the sampling frequencies are hours, days and weeks (at most 1-2 weeks); the methods calculated by using the travel distance and time of the tracer chemical. It was reported that the quantitative methods gave wrong results by different studies. One of the quantitative methods is the one offered by Kirkpatrick and Wilson (1989). In this method, by using the equation below, the time of the peek concentration of the tracer is determined. The sampling frequency is determined by dividing the test time by 30.

$$t_p = 2.78x10^{-4}\frac{L}{v_p} \qquad (1)$$

where L is the distance between the wells and υ_p is the velocity.

The amount of the chemical and the sampling frequency used in this project was determined by EHTD method offered by Field (2003). This method depends on the solution of the equation 7.2 shown below.

$$R_d\frac{\partial C}{\partial t} = D_z\frac{\partial^2 C}{\partial z^2} - \upsilon\frac{\partial C}{\partial z} - \mu z \qquad (2)$$

Where R_d is dimensionless dissolving factor, C is concentration, t is time, D_z is axial diffusion constant, υ is the average velocity, μ is dissolver viscosity. In this equation, the assumptions are such that the tracer is injected as a slug and it is assumed that no reaction takes place. For the other boundary conditions such as continuous injection, Field (2003) offered different solutions.

$$f(x^*) = C_p - \frac{M}{An_e\sqrt{4\pi D_z t_p}} \qquad (3)$$

In order to use the equation above the mass of the tracer chemical, M, flow rate Q, porosity, n_e, axial dispersivity D_z, area A and the peek concentration time, t_p, should be known. Field used the functional dependence of these parameters on flow rate and travel time in order to determine the tracer concentration, tracer mass and axial dispersivity by using the tank reactor mixing continuously. For the unknown parameters, correlations were used.

Using the EHTD method and assuming that *fluoreiscein* will be injected from re-injection well (MTA – 1) with a flow rate of 40 l/s, for a 50m thickness reservoir formation with 8.0% porosity for a well separation of 100 m, 1.53 kg tracer chemical must be injected. It was assumed that the tracer will be injected for 4 hours. The expected values of chemical concentration and sampling frequency (circles) are shown in Fig. 8.

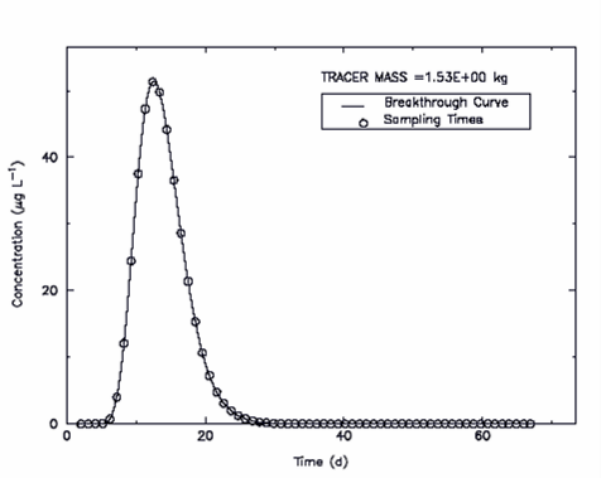

Figure 8. The expected values of chemical concentration and sampling frequency

Implementation of Tracer Test

The flow rate, temperature and dynamic level measurements were made in production and re-injection wells. Flow rates were measured using a Danfoss 3000 magnetic flow meter. Temperatures were measured using a thermometer. Static and dynamic levels in production wells were measured using nitrogen injection lines. Wellhead of MTA-1 well was modified for tracer test. All production well heads were prepared for sample collection purposes.

Using ½" and 1" valves after pump discharged head before the control valves. 1.53kg Fluorescein was mixed with 20kg water and then injected into MTA – 1 well in nearly 6 minutes. Prior to the tracer test calibration samples were collected from each well. After that samples were collected in 0.5 liter sample bottles. The fluorescein concentration was detected by using Turner Quantech Fluorimeter. Samples were placed in 3.5 ml Suprasil quartz cuvettes and a 490 nm narrow band excitation filter was used in measurements. First a calibration fluid is prepared for different concentrations (i.e. 1, 2, 4, 8, 10, 20, 30, 40 and 50 ppb). Following that a calibration run is conducted. A regression constant, larger than 0.9, was used in all measurements. Following that samples were placed in round 3.5 ml cuvettes and measurements were conducted. Calibration was repeated each day as the fluorimeter required re-calibration once the device is turned off.

Tracer Analysis

Tracer Models

Tracer test data measured was analyzed using multi fracture, single fracture, uniform porous (1-D and 2-D), fracture-matrix, double porosity pseudo steady state, double porosity cubes and double porosity slabs models (Akin, 2001). The models were matched to field data using non-linear-least-squares approximation. Microsoft Excel Solver uses the Generalized Reduced Gradient (GRG2) nonlinear optimization code developed by Lasdon and Waren (Fylstra et al. 1998). By minimizing the following objective function R, the parameters of the proposed analytical transfer functions can be estimated.

$$R = \sum_{i=1}^{n} w_i (C_{\mathrm{mod}\,el} - C_{\mathrm{exp}\,eriment})^2 \qquad (4)$$

Here w_i' s are the inverses of the variances of the experimental measurement errors, which will give the maximum-likelihood/minimum-variance estimates of the parameters (Akin, 2001).

The flow of tracer between an injection and a production well pair has been described both analytically and numerically by a number of authors. In this study, six different models were considered: multi-fracture model, fracture-matrix model, uniform porous model, double porosity slabs model, double porosity cubes model, and double porosity pseudo steady state model. In each model it is assumed that there is a good connection between the injection and production wells along a streamline which is surrounded by a stream tube of constant cross section. The tracer is injected as a slug from the injection well and the response is recorded in the observation well (Akin, 2001). The description of each model is given below.

Multi-Fracture Model

This model, as reported by Fossum and Horne (1982), assumes a single/multi fracture system, joining the injection and observation wells. Dispersion is due to the high velocity profile across the fracture and molecular diffusion, which moves tracer particles between streamlines (Taylor dispersion). The transfer function C_t is given by the following expression:

$$\mathrm{C_t} = \sum_{\mathrm{i=1}}^{\mathrm{n}} \mathrm{e_i C_r}(R_\mathrm{i}/u_\mathrm{i}, \mathrm{P_{ei}}) \qquad (5)$$

Here n is number of flow channels in the fracture system, e_i is the flow contribution coefficient, R_i is the apparent fracture length, u_i is the velocity, and P_{ei} is the Peclet number of the i^{th} flow channel. Therefore if "n" is taken as one then only a single fracture is present. It should be noted that for all practical purposes, a multi fracture system must be represented with at least two fractures, since the value of the transfer function, C_t, does not change much as "n" increases (Akin, 2001).

The form of C_r for each of the paths for a mass of tracer concentrated at point x=0 at time=0 is

$$\mathrm{C_r} = L \frac{1}{\sqrt{t}} \frac{2t_m}{t} Exp\left(\frac{-P_e (t - \mathrm{t}_m)^2}{4 t_m t} \right) \qquad (6)$$

Here P_e is a Peclet number corresponding to the ratio of tracer transport by advection to tracer transport by diffusion, t_m is the mean arrival time (seconds) and L is a model parameter. Using the above model and by knowing the distance between the injector and producer, R, it is possible to obtain m, the mass of tracer entering the stream tube, the dispersion coefficient for each flow channel by using the following definition:

$$D_{tr} = \frac{R^2}{P_e t_m} \qquad (8)$$

It should be noted that the above model could also be used together with other models.

Fracture-Matrix Model

In this model, as reported by Bullivant and O'Sullivan (1989), there is a large fracture with micro fracturing in the rock matrix on either side. Tracer particles leave the main fracture and enter the micro fracture network (there is a small amount of fluid exchange), stay for a while, and then return to the main fracture.

Longitudinal dispersion due to the velocity profile across the fracture is ignored in order to give a clear

distinction from the single fracture model. A fracture with fluid velocity constant across the thickness and with diffusion perpendicular to the fracture into an infinite porous medium is used in this model. The solution is in the following form:

$$C_r = JU(t-t_b)^{-1/2} Exp\frac{-t_b}{w(t-t_b)} \qquad (7)$$

Here U is the Heaviside step distribution, w is a ratio of transport along the fracture to transport out of the fracture, t_b is the response start time, and J is a model parameter, w is peclet number.

Uniform Porous Model

In the uniform, homogeneous porous model, it is assumed that a slug of tracer is instantaneously injected into a system with constant thickness. It is also assumed that, the flow is rapid allowing the kinematic dispersion components to be predominant (For purely hydrodispersive transfer the solution for one-dimensional flow as reported by Sauty (1980) is,

$$C_r = \frac{K}{\sqrt{t_r}} Exp(-\frac{P_e}{4t_r}(1-t_r)^2) \qquad (8)$$

where

$$K = \sqrt{t_{rm}} Exp(\frac{P_e}{4t_{rm}}(1-t_{rm})^2) \qquad (9)$$

$$t_{rm} = \sqrt{1+P_e^{-2}} - P_e^{-1} \qquad (10)$$

In the above equations P_e is the dimensionless Peclet number and t_r is the mean arrival time, K is model parameter. Similarly, Sauty (1980) also reported an analytical expression for the slug injection of a tracer solution into a two dimensional field. The solution on the flow axis can be obtained similar to the one-dimensional form as shown below.

$$C_r = \frac{K}{t_r} Exp(-\frac{P_e}{4t_r}(1-t_r)^2) \qquad (11)$$

where

$$K = t_{rm} Exp(\frac{P_e}{4t_{rm}}(1-t_{rm})^2) \qquad (12)$$

$$t_{rm} = \sqrt{1+4P_e^{-2}} - 2P_e^{-1} \qquad (13)$$

Double Porosity Slabs Model

The double-porosity slabs model has parallel fractures with constant thickness a, separated by slabs of the rock matrix giving a constant separation b (Bullivant and O'Sullivan, 1989).

Tracer movement in slabs is modeled by diffusion perpendicular to the fractures. If the ratio of transport along the fracture to transport out of the fracture, w, the response start time, t_b, the matrix block fill up time, t_f, and the model parameter, J, and the injection rate, Q are known, the mass of tracer, m, p is Laplace inversion parameters and the ratio of fracture porosity, ϕ_f to matrix porosity ϕ_m can be estimated using the equation given below.

$$C_r = JExp(-t_b(2\sqrt{\frac{p}{wt_b}}\tanh(\frac{t_f}{2}\sqrt{\frac{p}{wt_b}})+p)) \qquad (14)$$

Here p is the Laplace transform parameter.

Double Porosity Cubes Model

In the double-porosity cubes model as reported by Bullivant and O'Sullivan (1989), it is assumed that the rock matrix consists of cubic blocks of side b separated by high permeability fractures of aperture "a".

The double-porosity cubes model differs from the double-porosity slabs model because for the cubes model, the area of the surface a distance b/2+z from the nearest fracture is proportional to the square of z, whereas for the slabs model the area of the surface a distance b/2-z from the nearest fracture does not vary with z. This affects the way tracer diffuses into the block. Tracer movement in the blocks is modeled by diffusion perpendicular to the nearest face. The solution is given by the following equation:

$$C_r = JExp(-t_b(2\sqrt{\frac{p}{wt_b}}\coth(\frac{t_f}{2}\sqrt{\frac{p}{wt_b}})-\frac{4}{t_f}+p)) \qquad (15)$$

Double Porosity Pseudo Steady State Model

For this model, the reservoir contains uniformly distributed high permeability micro fractures which divide the reservoir into low permeability blocks that consist of unswept pores by the fluid flow.

Similar to the mechanism defined for the fracture-matrix model, the tracer leaves the micro fractures

and then returns again. However the effect is different, such that the blocks may be filled with tracer. Longitudinal dispersion due to the movement of fluid into the micro fracture network is neglected. The solution for this case is reported by Bullivant and O'Sullivan (1989) and given below. In this equation, α_m matrix porosity, and α_f is fracture veloncity.

$$C_r = JExp(-\alpha_m t)U(t-t_b)^{1/2} I_1(2(t_b \alpha_f \alpha_m (t-t_b))^{1/2}) \quad (16)$$

In the above equation a_f is the rate of tracer interchange per unit fracture volume and α_m is the rate of tracer interchange per unit matrix volume.

RESULTS AND DISCUSSIONS

Tracer concentration time plots were analyzed using the aforementioned mathematical models. Sum of squares residual values were used to identify the best matching model for the tracer return curves reported for Fethibey and MTA-2 wells (Fig. 9 and 10). The tracer data obtained from other wells are not analyzable as concentration data are limited. The smallest sum of squares residuals was obtained using the multi-fracture model using three fractures for both wells. The uniform porous models were not as successful as the other models. Moreover, they are not physically representative of the Kızılcahamam field since the formation is believed to be fractured. Like wise double porosity models (i.e. double porosity cubes and slabs and double porosity pseudo steady state) and the fracture matrix models are physically not representative since they assume that flow occurs both in fracture and the matrix. However, as stated above, the producing formation in Kızılcahamam field is fractured both the matrix permeability is known to be very small (Gevrek, 2000). In this regard, single fracture and multi-fracture models are the only models that physically represent the field. Of these models, single fracture model assumes that only one apparent fracture connects the injection well and the producing well. Since the sum of square residuals obtained using this model were less than the ones obtained using the multi-fracture model, the multi fracture model is chosen as the best representing the fast flows occurring in the field. These results show that Kızılcahamam field is not homogeneous field that can be represented using simple homogeneous models such as uniform porous models and single fracture model. The results of the tracer analyses are reported in Table 2 and 3 for each virtual fracture.

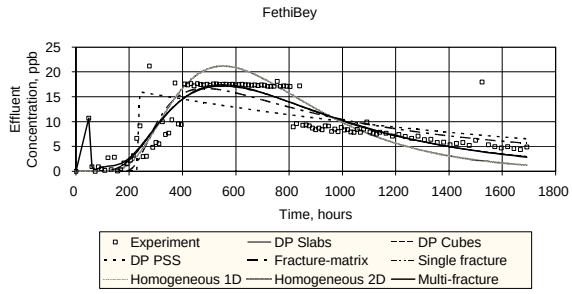

Figure 9. Fethibey tracer match.

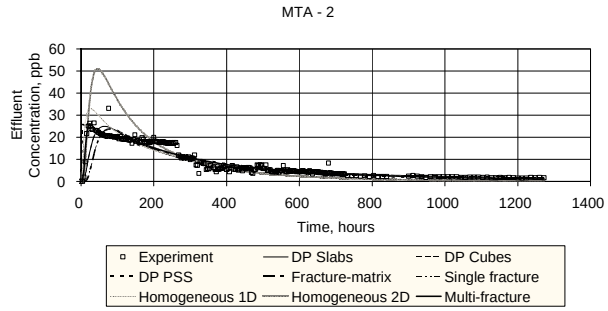

Figure 10. MTA-2 tracer match.

Table 2. Fethi Bey tracer matching parameters

Peclet number	Fracture Length(m)	Mean arrival time (hrs)	% contribution	D_l, dispersion m^2	U, m/hrs
70.61	7425.20	40.33	0.01	56.19	9.92
5.44	968.97	932.70	0.18	31.52	0.43
15.20	6.11	146.92	0.81	71.64	2.72
				Apparent velocity	**4.36**

Table 3. MTA-2 tracer matching parameters

Peclet number	Fracture Length(m)	Mean arrival time (hrs)	% contribution	D_l, dispersion m^2	U, m/hrs
50.92	0.41	46.24	0.07	0.38	0.65
1.44	529.47	624.59	0.10	1.00	0.05
1.77	49.73	89.93	0.83	5.66	0.33
				Apparent velocity	**0.35**

CONCLUSIONS

1. The largest temperature drop since re-injection from MTA-1 is observed in IHL-1. However, it is believed that a cold water zone encroachment is responsible due to cement failure or mechanical problems (casing failure) in the wellbore.
2. Although a re-injection scheme is applied in the Kızılcahamam geothermal field a decline in pressure is still observed while the temperature drop is insignificant.
3. Total production to re-injection ratio was found as 3.2 . This ratio is relatively high for a low temperature geothermal field and this shows that pressure decline is more than it should be.
4. The interpretation of tracer test shows that there is communication between re-injection well (MTA-1) and other wells in the field.
5. Multifracture tracer model with three fractures is the most suitable model to describe the Kızılcahamam low temperature geothermal field.
6. Kızılcahamam field is not a homogeneous field that can be represented using simple homogeneous models such as uniform porous models and single fracture model.

REFERENCES

Akin, S. (2001) "Analysis of Tracer Tests with Simple Spreadsheet Models" *Computers & Geosciences*, 27, 2, 171-178.

Bullivant, D.P., O'Sullivan, M.J., (1989). "Matching a field tracer test with some simple models." *Water Resources Research* 25 (8), 1879±1891.

Demirorer, M. (1985). "Ankara-Kızılcahamam rezistivite etudu", in Turkish, *MTA Report* No. 7781.

Erol, O. (1955). "Koroglu Isıkdaglari volkanik kutlesinin orta bolumleri ile Beypazari-Ayas arasindaki Neojen havzasinin jeolojisi hakkinda rapor (in Turkish)" MTA Report No: 2299.

Field M. S. (2003). "A review of some tracer-test design equations for tracer-mass estimation and sample-collection frequency." *Environ Geol* 43 (8): 867-881.

Fossum, M.P., Horne, R.N., (1982). "Interpretation of tracer return profiles at Wairakei geothermal field using fracture analysis." *Geothermal Resources Council, Transactions* 6, 261±264.

Fylstra, D., Lasdon, L., Watson, J., Waren, A., (1998). Design and use of the Microsoft Excel Solver. *Interfaces* 28 (5), 29±55.

Gevrek, A.I. (2000) "Water/rock interaction in the Kizilcahamam Geothermal Field, Galatian Volcanic Province (Turkey): a modelling study of a geothermal system for re-injection well locations", *Journal of Volcanology and Geothermal Research*, **96** (3-4), 207-213.

Gevrek, A.I., Aydin, S.N. (1988). "Hydrothermal alteration studies in Kızılcahamam Ankara geothermal field and its evolution on the development of this field. In: *Proc. Int. Mediterranean Congress on Solar and Other New-Renewable Energy Resources*, 14–19 Nov., Antalya. pp. 609–616.

Gulec, N (1994) "Geochemistry of thermal waters and its relation to the volcanism in the Kizilcahamam (Ankara) area, Turkey" *Journal of Volcanology and Geothermal Research*, **59**, 4, 295-312.

Gurer, A., Celik, I. (1987). "Kızılcahamam ve c¸evresinin sismik etudu" in Turkish, *MTA Report* No. 8766.

Kaya, T. (2005) "Characterization of Kizilcahamam geothermal field by tracer testing", Msc Thesis, Middle East Technical University.

Kilpatrick ,F. A., (1993). "Simulation of Soluble Waste Transport and Buildup in Surface Waters Using Tracers." T*ech.Rep.Techniques of Water-Resources Investigations*, Book 3, Chapter A20,37 p., U.S. Geological Survey.

Kilpatrick ,F. A., Wilson Jr.,J.F., (1989). "Measurement of Time of Travel in Streams by Dye Tracing." *Tech. Rep.27 Techniques of Water-Resources Investigations of the U.S. Geological Survey*, Book 3, Chapter A9, 27 p., U.S. Geological Survey.

Kocak, A. (1977)."Kızılcahamam kaplicasi hidrojeolojisi etudu" in Turkish, *MTA Report* No. 5669.

Ongur, T. (1976). "Kızılcahamam, Camlidere, Celtikci ve Kazan dolayinin jeolojisi ve jeotermal enerji olanaklari", in Turkish, *MTA Report* No. 5669.

Ozbek, T. (1988). "Interpretation of Ankara-Kizilcahamam geothermal area." *U.N. Seminar on New Developments in Geothermal Energy*, 22-25 May 1989, Ankara.

Sauty, J.P., (1980). "An analysis of hydrodispersive transfer in aquifers". *Water Resources Research* 16 (1), 145±158.

Tatli, S. (1975). "Kızılcahamam dogu alani jeolojisi ve jeotermal enerji olanaklari", in Turkish, *MTA Report* No. 5749.